(2)

AD-A224 822

DOUBLE DIFFUSIVE INTERLEAVING ACROSS A THERMOHALINE FRONT

FINAL REPORT TO THE OFFICE OF NAVAL RESEARCH

UNDER CONTRACT N00014-87-K-0390

Eric S. Posmentier
~~Southampton College~~
Long Island University
Southampton NY 11968

30 May, 1990

ABSTRACT

A model of double diffusively driven interleaving layers across a thermohaline, barotropic front is developed. The mechanism of the interleaving was proposed by Stern (1967) for small perturbations of continuous, large scale T-S gradients in the saltfingering regime by double diffusive interleaving. The model shows that this mechanism is also effective for interleaving across an initially sharp front, after strong T-S inversions develop between intrusions, in regions in which the mean vertical gradients are in the saltfingering, diffusive, or doubly stable regimes.

The vertical scale of the intrusions increases with increasing cross-frontal T-S discontinuities, and decreases with increasing mean vertical density gradients. The cross-frontal fluxes caused by the finescale interleaving can be substantial, and the vertical finescale fluxes can be up gradient. Sensitivity studies are performed to study the effects of the mean gradients, microscale flux parameters, and intrusion thickness and tilt on the interleaving T-S signature, velocity and length.

I. INTRODUCTION

In regions with large scale epipycnal T-S gradients and with diapycnal gradients suitable for salt fingering, the salt fingering drives double diffusive finescale interleaving (DDI) which undergoes unstable growth. Stern (1967) developed an analytic perturbation solution for this phenomenon. Advection along the large scale epipycnal gradients causes alternate layers of DDI to become relatively warm and salty. The thermohaline properties of these layers cause a divergence of the vertical flux of buoyancy by salt fingering, and they gain buoyancy. If the layers are slightly tilted with respect to horizontal, their buoyancy anomaly will lead to an acceleration of the advection, thus closing the positive feedback loop of unstable growth.

Many observations of DDI have been made in a variety of regions, and Stern's (1967) model has frequently been invoked as a possible explanation of the observations. For example, Joyce et al (1978) observed DDI across the Antarctic Polar Front; Hallock (1985) found DDI in the Norwegian Sea; and Posmentier and Houghton (1978) observed DDI across the shelf/slope front of the Middle Atlantic Bight. However, there were two significant gaps between Stern's (1967) explanation and these observations: (1) Stern's explanation applies to DDI in regions of continuous gradients, not necessarily to cross-frontal DDI, and (2) Stern's explanation applies directly only to the initial instability before the initial vertical gradients become significantly perturbed, not necessarily to the later stages after temperature

and salinity inversions are present.

Toole and Georgi (1981) added viscosity to Stern's (1967) model, and found the solutions to be qualitatively unchanged although the DDI developed less rapidly. They also noted, as did Posmentier and Hibbard (1982), that an "optimum" tilt of the intrusive layers would cause a maximum growth rate of the DDI. Posmentier and Hibbard (1982) investigated these optimum tilts and found that the tilt component parallel to the mean epipycnal gradients had relatively little effect on the growth rate of DDI, and that positive growth was possible with along-gradients tilts of either sign. However, the cross-gradient tilt was found to be critical to growth rate.

Posmentier and Hibbard (1982) also found that very large epipycnal and diapycnal fluxes of salt, heat, and buoyancy are caused by the DDI, and suggested that these large fluxes might play a role in larger scale structures. Posmentier and Kirwan (1985) hypothesized that these large fluxes caused by DDI can act to enhance the temperature, salinity, and buoyancy signatures of some mesoscale structures. They presented quantitative examples for a warm and a cold core mesoscale ring to demonstrate the feasibility of the hypothesis. The gap between Stern's (1967) mechanism and the frontal regions to which it was being applied, however, remained an unresolved issue.

McDougall (1985a, 1985b) suggested a model which moves toward removing the limitations of the perturbation assumptions. The model he proposed is an alternating slabs model, rather than the continuous harmonic function of space upon which the earlier work had been based. It was demonstrated that if the temperature

and salinity discontinuities between successive slabs are initially all equal, the system will be unstable with respect to temperature and salinity perturbations of opposite signs in alternate layers. The growth mechanism is identical to that originally proposed by Stern (1967). However, these perturbations can continue to grow beyond small amplitudes until temperature or salinity inversions occur. Furthermore, it was shown that a steady state solution exists for DDI after the inversions have become established. However, this model was no more applicable to fronts than was Stern's (1967) earlier model.

Turner (1978) proposed a mechanism similar to Stern's (1967) to explain both laboratory and oceanic observations of cross-frontal DDI. This was elaborated upon by Ruddick and Turner (1979), who also explained the dependence of the vertical scale of the DDI on the cross-frontal thermohaline gradients and on the vertical density gradient. In these models, however, the earth's rotation was neglected, so their results can be applied to oceanographic observations only by extrapolation.

In this paper, a model of double diffusively driven interleaving across a vertical, thermohaline, barotropic front is formulated. One purpose of the model is to demonstrate that the original mechanism proposed by Stern (1967) can produce such DDI, even though the original theory and its extensions were not directly applicable either to fronts or to interleaving in which the vertical salinity and temperature gradients were perturbed beyond small amplitudes. The second purpose is to demonstrate that all these solutions exist not only for large scale

environments which are conducive to salt fingering, but also in regions with T and S both decreasing upward, and in doubly stable regions. Third, the model will be used to evaluate several observable and significant properties of cross-frontal DDI, such as horizontal length scales, strength of the salinity and temperature variations, and cross-frontal fluxes caused by the DDI. Finally, the model will be used to evaluate the sensitivity of cross-frontal DDI to the hydrographic features of the front, to the parameters controlling vertical microscale (saltfingering and diffusive) fluxes, and to the vertical thickness and tilts of the layers.

II. FORMULATION OF THE MODEL

A. Structure and Form

The front and its environment, before the front is disturbed by intrusions, consists of two vertically-stratified regions with the same vertical gradients of salinity, temperature and density, S_z, T_z, and ρ_z, respectively. The vertical front is in the plane $x=0$ in the x(east), y(north), z(down) coordinate system. There is a discontinuity in both salinity and temperature, of S_1 and T_1, respectively, crossing the front from the $x<0$ side to the $x>0$ side, but no discontinuity in density. The ambient conditions are described by $S=S_0-S_1+S_z z$, $T=T_0-T_1+T_z z$, and $\rho=\rho_0+\rho_z z$ for $x<0$, the cold fresh (CF) side of the front, and by $S=S_0-S_1+S_z z$, $T=T_0-T_1+T_z z$, and $\rho=\rho_0+\rho_z z$ for $x>0$, the warm salty (WS) side of the front.

The front's shape is changed by a series of equally thick, parallel, tilted slabs of water moving in opposite directions

(Fig. 1). The even-numbered slabs carry CF water a distance 2L in the positive x-direction, and the odd-numbered slabs bring WS water in the opposite direction. Microscale double diffusive fluxes of salt and heat between adjacent layers release potential energy and change the densities of the layers, causing pressure gradients which drive the finescale interleaving motion. The layers are separated by planes of constant kx+hy+z, and the value of the plane's constant is (j-½)H at the top of the j'th layer, where H represents the layers' thickness.

The x-, y-, and z-components of velocity in the CF layers are U, V, and W. In the WS layers, they are -U, -V, and -W. One condition for the validity of the solution for velocity is that U must be positive. The salinity, temperature, and density in the CF n'th layer (in this report, n is always used to denote an even integer) are

$$S=S_0-S_1+nHS_z+S_x x+S_y y-S' \quad (1)$$

$$T=T_0-T_1+nHT_z+T_x x+T_y y-T' \quad (2)$$

$$\rho=\rho_0+nH\rho_z+\rho_x x+\rho_y y-\rho' \quad (3)$$

In the n+1'st layer (which is WS), they are

$$S=S_0+S_1+nHS_z+S_x x+S_y y+S' \quad (4)$$

$$T=T_0+T_1+nHT_z+T_x x+T_y y+T' \quad (5)$$

$$\rho=\rho_0+nH\rho_z+\rho_x x+\rho_y y+\rho' \quad (6)$$

A linear equation of state is used, so

$$\rho_x=\beta S_x-\alpha T_x \quad (7)$$

$$\rho_y=\beta S_y-\alpha T_y \quad (8)$$

$$\rho_z=\beta S_z-\alpha T_z \quad (9)$$

$$\rho'=\beta S'-\alpha T' \quad (10)$$

$$0=\beta S_1-\alpha T_1 \qquad (11)$$

where β is the coefficient of haline contraction, and α is the coefficient of thermal expansion.

B. Boundary Conditions

The water entering a CF layer at x=-L is water from the adjacent ambient environment in the vertical range of 2H centered a distance H' below the center of the CF layer. Similarly, the water entering a WS layer at x=+L is water from the adjacent ambient environment in the vertical range of 2H centered a distance H' above the center of the WS layer. The process at the origin of the CF layers, at x=-L, leads to the following boundary conditions:

$$-S_xL-S'=S_zkL+S_zH', \text{ and } S_y=-hS_z \qquad (12,13)$$

$$-T_xL-T'=T_zkL+T_zH', \text{ and } T_y=-hT_z \qquad (14,15)$$

$$-\rho_xL-\rho'=\rho_zkL+\rho_zH', \text{ and } \rho_y=-h\rho_z \qquad (16,17)$$

Eqs (16,17), however, are not independent. They follow from the four prior boundary condition equations and the equation of state. The boundary conditions arising from the process of WS layer formation at x=+L are redundant with those just given.

The differences in S, T, and ρ across the interfaces separating each CF layer from the WS layer above it, or below it, respectively are

$$S_{n-1}-S_n=2S_1-HS_z+2S' \text{ and } S_{n+1}-S_n=2S_1+HS_z+2S' \qquad (18,19)$$

$$T_{n-1}-T_n=2T_1-HT_z+2T' \text{ and } T_{n+1}-T_n=2T_1+HT_z+2T' \qquad (20,21)$$

$$\rho_{n-1}-\rho_n=2\rho_1-H\rho_z+2\rho' \text{ and } \rho_{n+1}-\rho_n=2\rho_1+H\rho_z+2\rho' \qquad (22,23)$$

Another condition for the validity of the results is that all the discontinuities in Eqs (18)-(21) must be positive, because the microscale flux laws to be introduced below are predicated on

this condition. Furthermore, stability requires that the density discontinuity in Eq (22) be negative, and in Eq (23) positive.

It is necessary that the vertical average of density over a range 2H should be the same immediately to the left of, and immediately to the right of x=+L. If this were not true, a horizontal pressure discontinuity would exist at x=+L which would increase ad infinitum with depth. At (x,y)=(L,y), the average density inside the n'th and n+1'st layer is $\rho_0+(n+\frac{1}{2})H\rho_z+\rho_x L+\rho_y y$. In the ambient water on the other side of the discontinuities at the layer ends and x=L, the average density over the same depth range is $\rho_0+\rho_z[(n+\frac{1}{2})H-kL-Hy]$. Equating these two average densities results in Eq (17) again, and in the new result

$$\rho_x=-k\rho_z \qquad (24)$$

A similar requirement at x=-L results in the two identical equations.

While the vertically-averaged pressure discontinuity across the planes x=+L and x=-L must be zero, the discontinuity across these planes is not zero if averaged only over those layers which are entraining ambient water and moving it toward x=0. The average pressure discontinuity at x=-L at the depths of the CF layers (and at x=+L at the WS layers), according to Bernoulli's Law, must be $\rho(U^2+V^2)$. It can be shown from the hydrostatic law that the pressure in the ambient fluid is

$$P=P_0+\rho_0 g(z-z_0)+\rho_z g(z^2-z_0^2)/2 \qquad (25)$$

where z_0 is the depth of the center of the n'th (CF) layer at x=-L, and P_0 is the pressure at that point. Now, if the ambient water in the depth range $z_0+H'-H$ to $z_0+H'+H$ is vertically mixed

before entering the CF layer, the pressure in this vertically-mixed ambient fluid, in which the density is $\rho_0+\rho_z(z_0+H')$, will be

$$P=P_0+\rho_0 g(z-z_0)+\rho_z g[2(z_0+H')(z-z_0)-(H+H')(H-H')]/2 \qquad (26)$$

if the pressure at the top (i.e., at $z_0+H'-H$) is the same as before mixing. On the other hand, the pressure inside the CF layer, which has the same density, will be

$$P=P_0+\rho_z g[2(z_0+H')(z-z_0)+(H+H'/4)H)]/2 \qquad (27)$$

if the pressure at the top is the same as in the ambient water. The difference between the pressures in Eqs (26) and (27), averaged over the depth range of the CF layer from $z_0-H/2$ to $z_0+H/2$, is

$$\bar{P}=\rho_z g(3H+2H')(H-2H')/8 \qquad (28)$$

According to Bernoulli's law, this pressure difference can be equated with the increase in kinetic energy per unit volume when the ambient water at rest acquires the velocity of the CF layer upon entering the layer. Thus,

$$\rho_z g(3H+2H')(H-2H')/8=[(\rho_0+\rho_z(z_0+H')](U^2+V^2) \qquad (29)$$

Neglecting the smaller part of the density on the right side of the Eq (29) results in the quadratic equation for H',

$$H'^2+HH'+(\rho_0(U^2+V^2)/\rho_z g-3H^2/4)=0 \qquad (30)$$

The same equation follows from the application of Bernoulli's Law to the pressure discontinuity at x=+L at the depths of the WS layers.

H' may also be related directly to the density anomaly in the WS layers by combining Eqs (16) and (24) to obtain

$$\rho'=-\rho_z H' \qquad (31)$$

C. Equations of Motion

In anticipation of applying Newton's Second Law to the dynamics of the layers, the pressure gradients within the layers can be derived from the hydrostatic law and the assumption that the gradients are equal and opposite in the n'th (even, CF) and n+1'st (odd, WS) layers:

$$\overline{(\partial P/\partial x)}_n=-gk\rho' \text{ and } \overline{(\partial P/\partial y)}_n=-gh\rho' \qquad (32,33)$$

$$\overline{(\partial P/\partial x)}_{n+1}=gk\rho' \text{ and } \overline{(\partial P/\partial y)}_{n+1}=gh\rho' \qquad (34,35)$$

where g is the acceleration of gravity. The equations of motion in the x- and y-directions respectively for the n'th layer, which are redundant with those for the n+1'st layer, are

$$gk\rho'+(-A/H)U+\rho fV=0 \qquad (36)$$

$$gh\rho'+(-A/H)V+(-\rho f)U=0 \qquad (37)$$

assuming that U and V are constants, where A is the viscosity and f is the Coriolis parameter. If the velocities are parallel to the planes separating the layers, the z-component of velocity must satisfy

$$W=-(kU+hV) \qquad (38)$$

D. Conservation Equations

The microscale flux laws governing the vertical fluxes of salt and heat between layers are required for the conservation equations. Assuming that saltfingering is the cause of microscale fluxes from the n-1'th (odd, WS) layer down to the n'th layer, the downward salt and heat fluxes across the interface is

$$F_S=\rho K(S_{n-1}-S_n) \text{ and } F_T=\tau(\beta/\alpha)\rho K(S_{n-1}-S_n) \qquad (39,40)$$

where K is the coefficient of diffusion for the salt fingering

interfaces, and τ is the ratio of density-equivalent heat to salt carried down by the salt fingering. If the interface below the n'th layer is a diffusive interface, the upward fluxes across this interface from the n+1'st layer below will be

$$F_S=\tau'(\alpha/\beta)\rho K'(T_{n+1}-T_n) \text{ and } F_T=\rho K'(T_{n+1}-T_n) \qquad (41,42)$$

If S and T are steady-state, the equations for conservation of salt and heat, respectively, in the n'th layer, after substituting Eqs (18-21) into (39-42) and adding advection terms, are

$$(K/H)(2S_1+2S'-HS_z)+(\alpha/\beta)(\tau'K'/H)(2T_1+2T'+HT_z) -US_x-VS_y=0 \qquad (43)$$

$$(\beta/\alpha)(\tau K/H)(2S_1+2S'-HS_z)+(K'/H)(2T_1+2T'+HT_z) -UT_x-VT_y=0 \qquad (44)$$

which are redundant with the equations for the n+1'st layer.

III. SOLUTION OF GOVERNING EQUATIONS

In the preceding section, twelve (12) constants and more or less arbitrary parameters have been used:

H S_1 S_z T_1 T_z K τ K' τ' A k $\dot{h}$

After substituting Eqs (12-15) into (43,44), there remain eight (8) unknowns:

S' T' ρ' U V W L H'

which appear in eight (8) independent, nonlinear equations:

10 30 31 36 37 38 43 44

The following pseudocode represents a procedure which may be used to solve the equations numerically.

Assign values to constants and parameters

Guess values of U and V

Solve (30) for H'

Do until H' stops changing:

Find ρ' from (31)

Find U, V, W from (36-38)

Solve (30) for H'; let new H'=average of old and new

End do loop

Find ρ' from (31)

Guess lower and upper bounds for L

Find S' and T' from (43,44) at each bound of L

Find corresponding ρ' values from (10)

Do until L stops changing:

Interpolate to new L at which ρ' agrees with (31)

Find ρ' at new L using (43,44) and then (10)

Replace one of bounds for L by new L

End do loop

Convergence occurs in only a few steps. However, for some values of the constants and parameters, convergence does not occur within reasonable bounds for L (for example, between 1 cm and 1000 km), or convergence occurs, but one or more of the assumptions mentioned in the preceding section (for example, U>0) is violated.

IV. NUMERICAL EXPERIMENTS

A number of numerical experiments were performed to demonstrate the existence of solutions for realistic constants and parameters, and to find the sensitivity of the solutions to the constants and parameters. The assumed values together with

results describing the solutions for 11 different experiments are summarized in Table 1.

Table 1. includes among the results the values of the salinity and temperature changes across the saltfingering interfaces between each WS layer and the CF layer immediately below it ($\Delta S+$ and $\Delta T+$, respectively), and of the diffusive interfaces between each WS layer and the CF layer above ($\Delta S-$ and $\Delta T-$). The magnitudes of these four discontinuities denote the "strength" of the DDI from the perspective of hydrographic data interpretation. Also included are the velocity components (U, V, W), the half-length of the intrusion (L), and the vertical displacement of ambient water being drawn into the interleaving layers (H'). In addition, the cross-frontal, horizontal salt fluxes (mg/cm^2-s) and heat fluxes (cal/cm^2-s) caused by the DDI, and the effective horizontal diffusion coefficients for salt and heat, K"S and K"T (cm^2/s), are included. The diffusion coefficients are defined here as the fluxes divided by the horizontal gradients in the frontal zone, S_1/L and T_1/L, respectively.

In all the numerical experiments, the constants:

α β S_0 T_0 g f

were set to

1.4E-4 7E-4 35 15 980 1E-4

respectively, in cgs units except for salinity, which is in mg/g.

Experiment A (see Table 1, column A) is used as a reference for comparison with the other experiments reported here. In this experiment, a front with a 1mg/g salinity discontinuity and a 5°C temperature discontinuity separates two regions with temperature

and salinity decreasing downward -- saltfingering regions. The 1000 cm thickness of the layers is typical of observed values (Posmentier and Houghton, 1978). The tilts are consistent with those discussed by Posmentier and Hibbard (1982). The values of the process-controlling parameters are representative of those generally discussed in the literature, if the interfaces between layers are 100 cm thick.

The results indicate that a solution exists: the mechanism under discussion can cause DDI under the conditions of experiment A, which are conditions not unlike those observed in various frontal regions. Furthermore, the results are comparable to DDI observed in such areas - the large S and T discontinuities across the saltfingering interfaces below the WS layers, and across the weaker diffusive interfaces above the WS layers, are detectable, and the total length of the layers (12.62km) makes their observation certain in any frontal field study.

The cross-frontal fluxes calculated by the model are substantial, and indicate that cross-frontal DDI may be an important factor in transport between water masses bounded by fronts. In addition, the vertical fluxes and salt and heat are upward, which is the upgradient direction. The effective coefficients of vertical diffusion are negative! The model thus lends qualitative support to the underlying assumption of Posmentier and Kirwan's counterintuitive hypothesis (1985) that DDI can amplify the contrast between contiguous water masses.

The advection of heat and salt into our out of each layer is exactly balanced by the microscale diffusion out of or into the

layer, as required by Eqs (43,44). In experiment A and most of the other experiments, the pressure gradient acceleration in the CF layers is oriented somewhat closer to the negative x-direction (out of the frontal region) than the y-direction (along front) because of the assumed components of tilt. The flow is roughly in geostrophic equilibrium, but viscosity is not negligible, so the velocity is aligned somewhat closer to the y-direction (along front) than the x-direction (cross front).

An additional set of experiments was performed in which the value of S_z was varied, keeping S_z and T_z both negative and the ratio S_z/T_z constant, so conditions remained favorable for saltfingering. In these experiments, DDI occurred only for $-S_z > -2.9E-5$ mg/g/cm. As the magnitudes of the vertical gradients were increased beyond this minimum, the strength of the interleaving increased relatively faster than the gradients, and L decreased less rapidly than the gradients' increases. Experiment B is an example of these effects. (See Table 1.) A further consequence of the increased vertical gradients in experiment B is the change in the range of H for which DDI occurred: $100 < H < 1390$ cm. The lower limit of H decreased considerably compared to experiment A, while the upper limit decreased very slightly.

The magnitudes of the cross-frontal discontinuities affect the results in the same sense as the vertical gradients, but not as strongly. (See experiment C in Table 1.) Interleaving occurs under the same conditions as experiment A but with different S_1 and T_1 (satisfying Eq (11), which states that the front is barotropic) only if $S_1 > 0.30$. However, doubling S_1 causes only

small increases in the strength of the stronger saltfingering interfaces, but causes near doubling of the salinity discontinuity and more than doubling of the temperature discontinuity in the weaker diffusive interfaces above the WS layers, making detection more likely.

A further consequence of the increased cross-frontal discontinuities in experiment C is that L nearly doubles, making it easier to find the intrusions. In addition, the range of H for which DDI occurs changes to $270<H<2990$ cm. The lower limit of H decreased very slightly compared to experiment A, while the upper limit doubled.

Changing the layer thickness from experiment A precluded DDI unless $2900<H<1460$ cm. Thicker layers (experiment D) tend to cause somewhat stronger saltfingering interfaces and longer intrusions, but cause the weaker diffusive interfaces to approach disappearance. It is particularly interesting that there is a definite range of values of H outside of which interleaving cannot occur, a phenomenon which is implicit in the literature but has not been explained previously.

The cross-frontal tilt of the layers, k, must satisfy $0.0094<|k|<0.0250$ for DDI to be possible without changing other parameters in experiment A. Doubling the magnitude of k (experiments E and F) causes a ninefold increase in δS^2 and an eighteenfold increase in δT^2, which are the least discernible of the discontinuities, thus making the interleaving much more noticeable in hydrographic sections or T-S diagrams. However, the doubling causes 2*L to decrease to 3.8 km, considerably

smaller than 2*L in experiment A, but still not difficult to locate in the field.

Changing the sign of k (experiment F) has the drastic effect of reducing U and L nearly to zero, making the intrusions too slow to be of any significance in causing cross-frontal fluxes and too slow to find in the field. This occurs because, if $k>0$, the cross-frontal velocity of the anomalously low density water entering the WS layers would cause them to sink. In order to rise, these layers must move predominantly in the y-direction, and are close to geostrophic. This defeats the basic mechanism which causes the interleaving, causing the layers to be only four times longer than their thickness.

The along-frontal tilt, h, is quite critical to the interleaving. If the value of h in experiment A is varied, DDI is still possible for $0.0018<-h<0.0230$ (h must remain negative.) The most significant effect of a larger tilt (see experiment G in Table 1) is the disproportionate increase in iS- and in iT-, the least discernible of the discontinuities, thus having the same effect as increasing the magnitude of k (experiment E) in making the interleaving much more noticeable in hydrographic sections or T-S diagrams. In addition, the flow is closer to geostrophic. Unlike increases in k, however, increasing h causes only a small decrease in 2*L.

DDI continues to occur if K in experiment A is varied in the range $0<K<.01$ cm^2/s. Reducing K (see experiment H) has the effect of increasing the strength of the intrusions, especially of the weak discontinuities across the diffusive interfaces above the WS layers. L, however, is reduced, but remains large enough

for the intrusions to be found in the field. The upper limit on K in the series of experiments including A and H should not be generalized, because all other parameters including k and h were kept constant in this particular sensitivity study, whereas in reality new values of k and h can permit DDI with K larger than the upper limit in this series of experiments.

In experiment I, τ was increased from experiment A. Other, similar experiments found DDI to occur for $0.51<\tau<1.0$. Larger values of τ have the same effect on the intrusions as smaller values of K. The action common to both increasing τ and decreasing K is that of decreasing the rate at which density in the WS layers is lowered by saltfingering downward into the CF layer below. This is the reason for their common effect on increasing the intrusion strength while decreasing intrusion length.

Changing the viscosity in experiment A within the range $0.019<A<0.8$ cm/s permitted DDI to occur. Experiment J shows that larger A causes the interleaving velocity to decrease only slightly in speed, while changing in direction towards the x-axis. This is because H' is required to increase, increasing á', which in turn increases the pressure gradients within the layers, offsetting most of the tendency to slow with increasing viscosity. At the same time, the velocity veers further from geostrophic towards counter gradient. Paradoxically, the interleaving strength increases (also because of the increase in H'), and 2*L is reduced.

In every experiment described so far, the ambient water

outside the interleaving region was in the saltfingering regime. Although this is a necessary condition for DDI in Stern's (1967) model for interleaving within a region with continuous gradients, it is not a necessary condition for cross-frontal interleaving. Ambient vertical gradients in the diffusive regime or in the doubly stable regime are also consistent with cross-frontal interleaving (the fourth possibility, doubly unstable, is of no interest.) In fact, experiments in these regimes suggest that interleaving is stronger and can occur over a wider range of the other parameters (S_1, h, K, etc.), than in the saltfingering regime. One example, experiment K, is included in Table 1. In this experiment, the magnitude (but not the sign) of T_z and the value of $á_z$ are the same as in experiment A, but S_z is changed. The interleaving is stronger than in any experiment except H, and 2*L, although smaller than in experiment A, is still not an impediment to finding intrusions in a field study.

V. CONCLUSIONS

1. A model extending the mechanism proposed by Stern (1967) is capable of explaining interleaving across thermohaline fronts, with alternating WS and CF layers separated by saltfingering and diffusive interfaces. The model's results and the observed features of cross-frontal DDI are quantitatively comparable.

2. Conclusion #1 applies to saltfingering regimes (regions with salinity and temperature gradients both directed upward), to diffusive regimes, and to doubly stable regimes.

3. The cross-frontal fluxes produced by DDI can be significant to salt and heat budgets of the water masses separated by the

front. The vertical components of the fluxes are up-gradient!

4. The upper bound of the range of possible vertical scales increases approximately in proportion to the cross-frontal salinity and temperature discontinuities, and decreases at the lower bound somewhat more slowly than the inverse of the vertical density gradient This is qualitatively consistent with the results of Ruddick and Turner (1979).

5. The strength of the DDI, as manifested by the magnitudes of the salinity and temperature discontinuities between layers, and the horizontal length scale, are sensitive to the vertical gradients, to the cross-frontal discontinuities, to the layer thickness and both components of tilt, and to the parameters controlling the saltfingering and double diffusion across the interfaces between layers.

REFERENCES

Hallock, Z.R., 1985. Variability of Frontal Structure in the Southern Norwegian Sea. J. Phys. Oceanogr. 15, 10, 1245-1254.

Joyce, T.M., W. Zenk, and J.M.Toole, 1978. An anatomy of the Antarctic polar front in the Drake Passage. J. Geophys. Res., 83, 6093-6113.

McDougall, T.J., 1985a. Double diffusive interleaving. Part I:linear stability analysis. J. Phys. Oceanogr., 15, 11, 1532-1541.

McDougall, T.J., 1985b. Double diffusive interleaving. Part

II:finite amplitude, steady state interleaving. J. Phys. Oceanogr., 15, 11, 1542-1556.

Posmentier, E.S., and A.D. Kirwan, 1985. The role of double diffusive interleaving in mesoscale dynamics: an hypothesis. J. Mar. Res., 43, 541-552.

Posmentier, E.S., and C.B. Hibbard, 1982. The role of tilt in double diffusive interleaving. J. Geophys. Res., 87, C1, 518-524.

Posmentier, E.S., and R.W. Houghton, 1978. Fine structure instabilities induced by double diffusion in the shelf/slope water front. J. Geophys. Res., 83, C10, 5135-5138.

Ruddick, B.R., and J.S. Turner, 1979. The vertical length scale of double-diffusive intrusions. Deep Sea Res., 26A, 903-913.

Stern, M.E., 1967. Lateral mixing of water masses. Deep Sea Res., 14, 747-753.

Toole, J.M., and D.T. Georgi, 1981. On the dynamics and effects of double-diffusively driven intrusions. Prog. Oceanogr., 10, 123-145.

Turner, J.S., 1978. Double diffusive intrusions into a density gradient. J. Geophys. Res., 83, 2887-2901.

TABLE 1. SUMMARY OF NUMERICAL EXPERIMENTS

	A	B	C	D	E	F
H(cm)	1000	1000	1000	1400	1000	1000
S1	0.5	0.5	1	0.5	0.5	0.5
T1(xC)	2.5	2.5	5	2.5	2.5	2.5
Sz(1/cm)	-4E-05	-1.6E-04	-4E-05	-4E-05	-4E-05	-4E-05
Tz(xC/cm)	-0.00068	-0.00272	-0.00068	-0.00068	-0.00068	-0.00068
K(cm/s)	0.01	0.01	0.01	0.01	0.01	0.01
g	0.56	0.56	0.56	0.56	0.56	0.56
K'(cm/s)	0.002	0.002	0.002	0.002	0.002	0.002
g'	0.56	0.56	0.56	0.56	0.56	0.56
A(cm/s)	0.02	0.02	0.02	0.02	0.02	0.02
k	-0.01	-0.01	-0.01	-0.01	-0.02	0.02
h	-0.004	-0.004	-0.004	-0.004	-0.004	-0.004
ΔS+	0.103	0.552	0.119	0.132	0.281	0.281
ΔT+(xC)	1.408	5.947	1.490	1.911	2.209	2.210
ΔS-	0.023	0.232	0.039	0.020	0.201	0.201
ΔT-(xC)	0.048	0.507	0.130	0.007	0.849	0.849
U(cm/s)	1.59	4.87	1.59	2.05	1.66	0.018
V(cm/s)	-2.46	-7.53	-2.46	-3.59	-4.04	4.37
W(cm/s)	0.0061	0.0185	0.0061	0.0062	0.0171	0.0171
L(km)	6.31	2.62	10.87	8.91	1.9	0.02
H'(cm)	430.8	329.3	430.8	601.8	338.9	338.9
S Flux	0.0501	0.9545	0.0628	0.0779	0.2000	0.0022
K"S	6.32E+04	5.00E+05	6.83E+04	1.39E+05	7.60E+04	8.68E+00
T Flux	0.5788	7.8577	0.6440	0.9830	1.2691	0.0138
K"T	1.46E+05	8.23E+05	1.40E+05	3.50E+05	9.64E+04	1.10E+01

(continued on next page)

TABLE 1. (continued)

	G	H	I	J	K
H(cm)	1000	1000	1000	1000	1000
S1	0.5	0.5	0.5	0.5	0.5
T1(xC)	2.5	2.5	2.5	2.5	2.5
Sz(1/cm)	-4E-05	-4E-05	-4E-05	-4E-05	2.32E-04
Tz(xC/cm)	-0.00068	-0.00068	-0.00068	-0.00068	0.00068
K(cm/s)	0.01	0.001	0.01	0.01	0.01
g	0.56	0.56	0.7	0.56	0.56
K'(cm/s)	0.002	0.002	0.002	0.002	0.002
g'	0.56	0.56	0.56	0.56	0.56
A(cm/s)	0.02	0.02	0.02	0.1	0.02
k	-0.01	-0.01	-0.01	-0.01	-0.01
h	-0.016	-0.004	-0.004	-0.004	-0.004
ΔS+	0.253	0.874	0.144	0.303	0.144
ΔT+(xC)	2.084	5.264	1.614	2.434	1.612
ΔS-	0.173	0.794	0.064	0.223	0.608
ΔT-(xC)	0.724	3.904	0.254	1.074	2.972
U(cm/s)	3.92	1.59	1.59	2.08	1.59
V(cm/s)	-1.5	-2.46	-2.46	-0.92	-2.46
W(cm/s)	0.0152	0.0061	0.0061	0.0171	0.0061
L(km)	5.15	0.98	4.47	2.15	1.84
H'(cm)	352.1	430.8	430.8	458.9	430.8
S Flux	0.4175	0.6630	0.0827	0.2735	0.2989
K"S	4.30E+05	1.30E+05	7.39E+04	1.18E+05	1.10E+05
T Flux	2.7518	3.6443	0.7425	1.8242	1.8221
K"T	5.67E+05	1.43E+05	1.33E+05	1.57E+05	1.34E+05

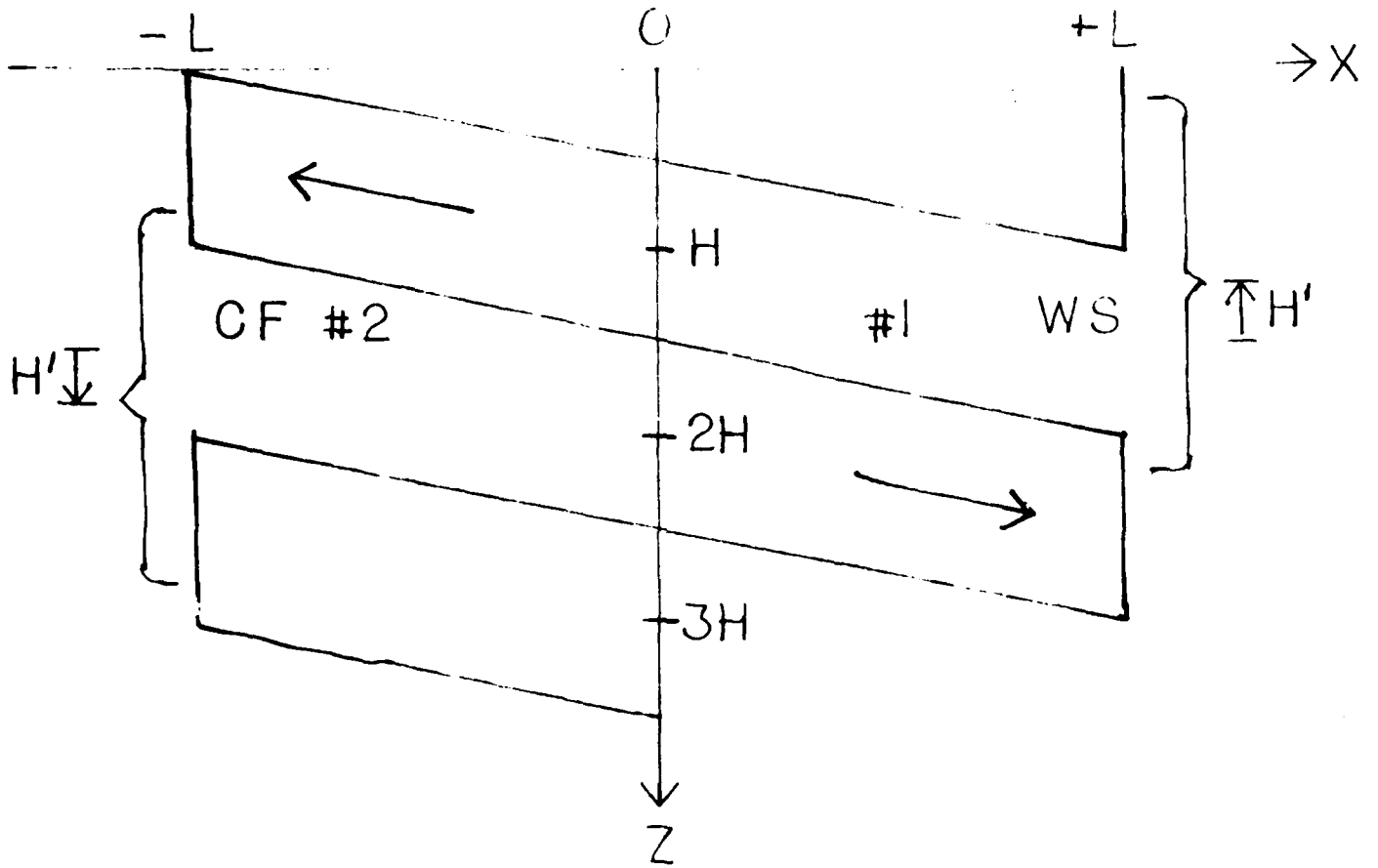

Figure 1

Geometric structure of

interleaving layers